

# Radiographic and metabolic evolution of prostate cancer lung metastasis detected by prostate-specific membrane antigen and fluoro-2-deoxy-D-glucose positron emission tomography/computed tomography

## ABSTRACT

We describe the case of a 75-year-old patient who progressed over a 12-year period from localized to symptomatic metastatic prostate cancer (PrCa) with lung as the sole organ of involvement. In this case, the specific sequence of positron emission tomography (PET)-based next-generation imaging with <sup>18</sup>F-sodium fluoride-, <sup>18</sup>F-fluoro-2-deoxy-D-glucose-, and <sup>18</sup>F-DCFPyL PET/computed tomography and biopsies allowed illustration of the pathway of disease progression from nonglycolytic hormone-sensitive PrCa to glycolytic castrate-resistant PrCa without neuroendocrine features. The observations provide a unique insight into the timelines of anatomical and metabolic progression of metastatic PrCa. They highlight the value of close radiographic surveillance of metastatic PrCa with modern imaging to guide early treatment interventions.

**Keywords:** Castrate-resistant prostate cancer, <sup>18</sup>F-DCFPyL, <sup>18</sup>F-fluoro-2-deoxy-D-glucose positron emission tomography, lung metastasis, positron emission tomography/computed tomography, prostate cancer, prostate-specific membrane antigen

## INTRODUCTION

Modern nuclear medicine imaging opens new avenues for observation of prostate cancer (PrCa) behavior and shows earlier points for intervention.<sup>[1]</sup> Prostate-specific membrane antigen (PSMA) positron emission tomography (PET) helps illustrate the complexity of the patterns of PrCa metastatic behavior.<sup>[2]</sup> On the other hand, incidental identification of PrCa metastasis by <sup>18</sup>F-fluoro-2-deoxy-D-glucose PET (FDG-PET), when other malignancies are suspected, provides new information on the patterns of metabolic progression of PrCa. Castrate-resistant prostate cancer (CRPC) progresses frequently from a non-glycolytic to glycolytic phenotype, a phenomenon that is associated with expression of glucose and monocarboxylate transporters<sup>[3,4]</sup> and has been frequently attributed to neuroendocrine differentiation.<sup>[2]</sup>

Despite such observations, the potential timelines of biochemical and radiographic progression of metastatic

hormone-sensitive prostate cancer (HSPC) and its transformation to CRPC, without or with glycolytic features,

**THEODOROS TSAKIRIDIS<sup>1,2,3</sup>,  
MICHAEL BONERT<sup>4,3</sup>, KATHERINE ZUKOTYNSKI<sup>5</sup>,  
ALEXANDER EFSTATHIOS ANAGNOSTOPOULOS<sup>6</sup>**

<sup>1</sup>Division of Radiation Oncology, Juravinski Cancer Center, <sup>4</sup>Department of Pathology, St. Joseph's Hospital, Departments of <sup>2</sup>Oncology, <sup>5</sup>Radiology and Medicine, <sup>3</sup>Pathology and Molecular Medicine and <sup>6</sup>School of Medicine, McMaster University, Hamilton, Ontario, Canada

**Address for correspondence:** Dr. Theodoros Tsakiridis, Radiation Oncology, Juravinski Cancer Center, 699 Concession Street, Hamilton, Ontario, L8V 5C2, Canada.  
E-mail: theos.tsakiridis@hhsc.ca

**Submitted:** 18-Feb-2020, **Revised:** 19-Mar-2020, **Accepted:** 31-Mar-2020, **Published:** 14-Sep-2020

This is an open access journal, and articles are distributed under the terms of the Creative Commons Attribution-NonCommercial-ShareAlike 4.0 License, which allows others to remix, tweak, and build upon the work non-commercially, as long as appropriate credit is given and the new creations are licensed under the identical terms.

**For reprints contact:** WKHLRPMedknow\_reprints@wolterskluwer.com

**How to cite this article:** Tsakiridis T, Bonert M, Zukotynski K, Anagnostopoulos AE. Radiographic and metabolic evolution of prostate cancer lung metastasis detected by prostate-specific membrane antigen and fluoro-2-deoxy-D-glucose positron emission tomography/computed tomography. World J Nucl Med 2020;19:421-4.

Access this article online	
<b>Website:</b> www.wjnm.org	<b>Quick Response Code</b> 
<b>DOI:</b> 10.4103/wjnm.WJNM_17_20	

remain poorly understood. Detection of such metastatic progression within a single organ, years after definitive local therapy, in the absence of local disease recurrence, presents a unique setting to understand better the natural history of metastatic PrCa and opens opportunities to study its unique biology.

We describe the case of a 75-year-old patient who developed a secondary rapidly progressing ipsilateral glycolytic CRPC metastasis 3 years after detection of a sole metastatic site of non-glycolytic HSPC in the left lung and 12 years after radical prostatectomy.

### CASE REPORT

At 63 years of age (2007), our patient was diagnosed with high-intermediate risk PrCa (Gleason score 7 (4 + 3), prostate-specific antigen [PSA]: 5.1 ng/ml). Baseline staging with computed tomography (CT) of the abdomen and pelvis showed a heterogeneous prostate gland and no evidence of extraprostatic extension or pelvic lymph node enlargement [Figure 1a], and he underwent laparoscopic prostatectomy with standard nodal dissection. Operative pathology indicated pT2c, N0, prostatic adenocarcinoma without lymphovascular or perineural invasion and led to undetectable PSA levels for 4 years (till 2011).

In 2012, PSA became detectable (0.11 ng/ml). Conventional imaging with CT of the abdomen and pelvis and <sup>18</sup>F-sodium fluoride (NaF)-PET/CT did not detect metastatic foci, and the patient was treated with standard salvage pelvic (4500 cGy) and prostatic bed boost (1980 cGy) radiotherapy with no biochemical response.

PSA continued to rise reaching 5ng/ml in early 2016 when imaging with CT and <sup>18</sup>F-NaF-PET/CT showed a solitary (2.0 cm × 1.8 cm) left lower lobe nodule [Figure 1b]. Due to the patient's previous smoking history, thoracic cancer was suspected and he was referred to a lung cancer diagnostic program. <sup>18</sup>F FDG-PET showed a minimally FDG-avid tumor [Figure 1c]. CT-guided biopsy proved PSA-expressing metastatic PrCa. He was started on androgen deprivation therapy (ADT), which produced PSAs of <1 ng/ml in the period 2017–2018. However, he progressed to CRPC in 2019 [Figure 2].

In January 2019, PSA rose to 13.26 ng/ml and he began developing shortness of breath. Repeat CT of the chest showed a new mass of 5.9 cm × 3.9 cm × 2.4 cm encasing

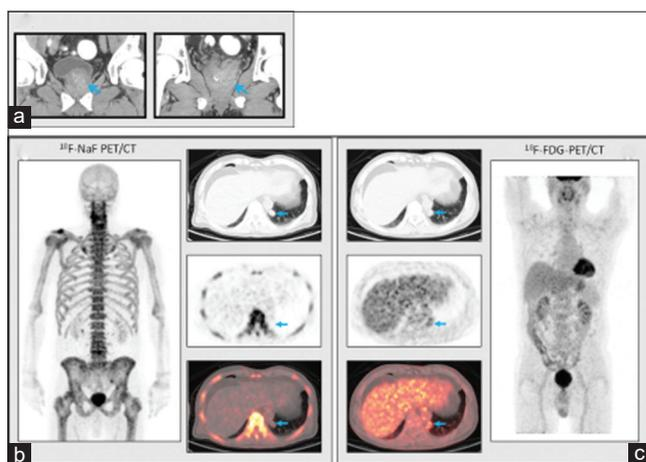


Figure 1: (a) In 2007, preoperative staging computed tomography of the abdomen and pelvis showed a heterogeneous prostate gland without evidence of extraprostatic extension or pelvic lymph node enlargement. (b) In early 2016, after failing salvage radiotherapy, prostate-specific antigen reached 5ng/ml, which led to repeat imaging. Computed tomography detected a new left lower lobe lung nodule but no evidence of disease in the pelvis. The nodule was biopsied and proved to be metastatic prostatic adenocarcinoma. <sup>18</sup>F-sodium fluoride positron emission tomography/computed tomography and (c) <sup>18</sup>F-fluoro-2-deoxy-D-glucose-positron emission tomography/computed tomography. Verified a solitary, minimally fluoro-2-deoxy-D-glucose-avid, left lower lobe nodule (blue arrows)

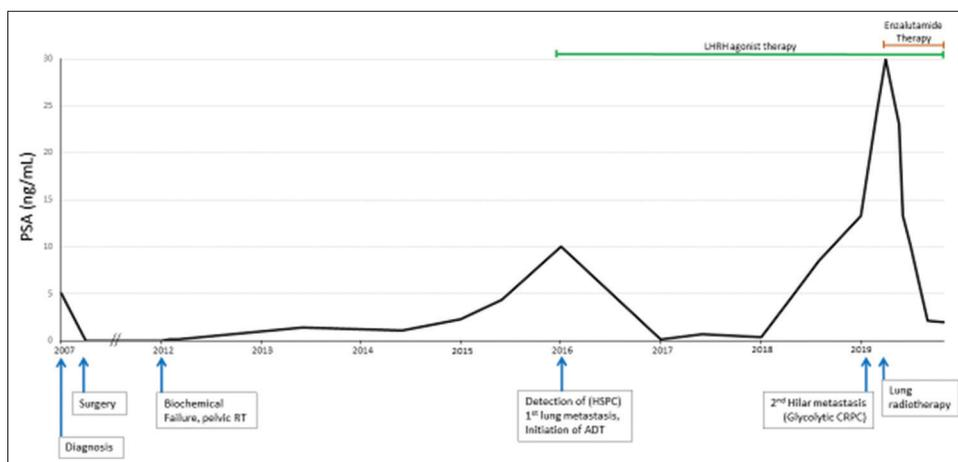


Figure 2: Prostate-specific antigen kinetics over the course of the disease. Arrows describe points of interventions

the left distal mainstem bronchus narrowing the airway. Once again, the radiographic features could not exclude lung malignancy.  $^{18}\text{F}$ -FDG-PET/CT showed that the primary left lower lobe nodule remained radiographically stable and was mildly FDG-avid [Figure 3]. However, the new left hilar mass was intensely FDG-avid raising the suspicion for *de novo* bronchogenic carcinoma [Figure 3].

Two months later, PSA increased to 24.22 ng/ml while on ADT. CT-guided biopsy of the left hilar mass showed histomorphology consistent with prostatic adenocarcinoma with mild-to-moderate anisonucleosis and gland formation. The disease was negative for neuroendocrine features (nuclear molding and scant cytoplasm). These findings were consistent with those found in the 2016 biopsy. Both tumors were positive for PSA and prostatic acid phosphatase and negative for thyroid transcription factor-1, CK7, napsin A, and CD56 [Figure 4].

$^{18}\text{F}$ -DCFPyL PET/CT showed that both the primary metastasis in the left lower lobe (detected in 2016) and the secondary hilar tumor (FDG avid, detected in 2019) were PSMA-avid [Figure 5]. There was no evidence of local prostatic bed recurrence, involvement of other organs, or skeletal metastasis throughout the course of his disease.

The pathologic and radiographic features of this case depicted oligometastatic CRPC, a setting where radiotherapy is being investigated. Our patient participated in a randomized trial investigating high-precision radiotherapy in

this setting (NCT02685397). Before treatment initiation, PSA reached 30 ng/ml. He was randomized to the radiotherapy arm and received hypofractionated radiotherapy to primary and secondary metastases in combination with enzalutamide and luteinizing hormone-releasing hormone agonist therapy. In early 2020, his PSA remained well-controlled [Figure 2].

## DISCUSSION

PrCa metastasis to multiple organs, including the lungs, is well-described,<sup>[5,6]</sup> but isolated lung metastasis from PrCa without concurrent bone or lymph node disease is fairly rare. Gago *et al.*<sup>[7]</sup> described three patients with isolated pulmonary lesions after radical prostatectomy. One patient underwent chemotherapy but died from his disease. The other two were treated with ADT therapy with either complete or partial response. Ciriaco *et al.* (2019) described 9 cases that underwent resection of lung metastases without preoperative ADT.<sup>[8]</sup> There are no reports describing the time-course of progression of isolated lung metastases from HSPC to CRPC in PrCa that remained confined to the lungs for over a decade.

The case presented here illustrates important features of metastatic PrCa behavior that points to a unique biology. It shows that PrCa can: (1) remain quiescent at metastatic sites for long periods of time before progressing biochemically, (2) show a slow progression and serial metastases within a single-organ site without evidence of skeletal involvement,

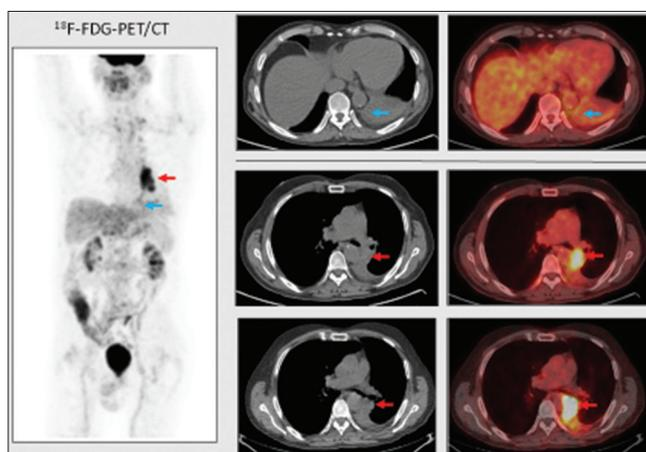


**Figure 3: Radiographic and metabolic progression of prostate cancer lung metastasis.** In January 2019, biochemical progression and development of shortness of breath led to restaging investigations.  $^{18}\text{F}$ -fluoro-2-deoxy-D-glucose-positron emission tomography/computed tomography showed that the primary left lower lobe nodule maintained minimal fluoro-2-deoxy-D-glucose avidity (blue arrows). A new, intensely fluoro-2-deoxy-D-glucose-avid, left hilar mass was detected indicating secondary metastasis and clonal metabolic progression to a glycolytic phenotype

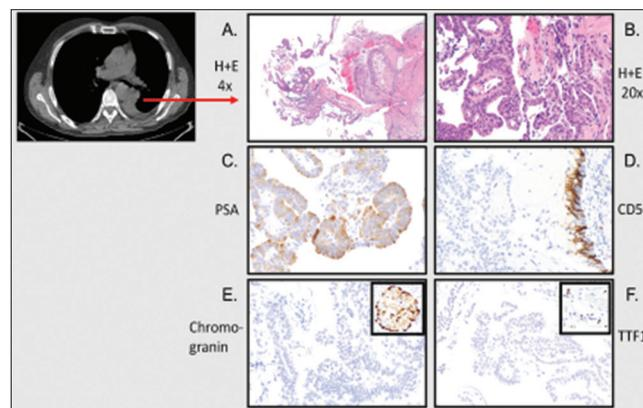


**Figure 4: Prostate cancer lung metastases can develop metabolic progression without neuroendocrine differentiation.** Computed tomography-guided biopsy (March 2019) of the left hilar mass showed morphology consistent with prostatic adenocarcinoma. The disease was negative for neuroendocrine features (nuclear molding and scant cytoplasm). The tumor was positive for prostate-specific antigen and prostatic acid phosphatase and negative for thyroid transcription factor-1, CK7, napsin A, and CDX2. Micrographs of the bronchial biopsy with selected immunostains are shown. (A)  $\times 4$  hematoxylin and eosin (H+E), (B) H+E  $\times 20$ , (C) prostate-specific antigen, (D) CD56, (E) chromogranin A, and (F) thyroid transcription factor-1. Insets for thyroid transcription factor-1 (F) and chromogranin A (E) positive controls. The CD56 immunostain (D) marked benign bronchial cells; the adenocarcinoma was negative for CD56

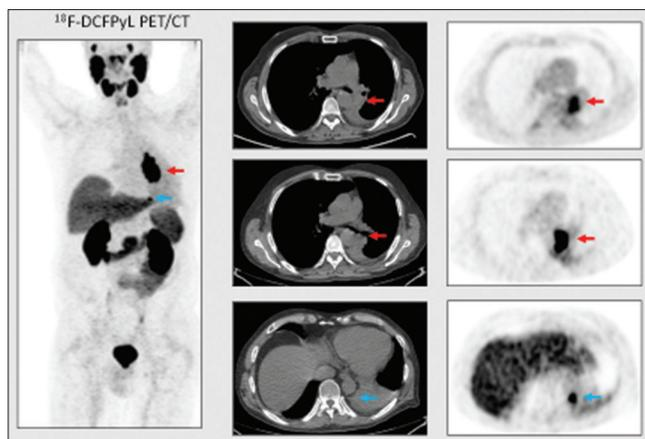


**Figure 5: Prostate cancer lung metastases can progress metabolically but remain prostate-specific membrane antigen avid.  $^{18}\text{F}$ -DCFPyL positron emission tomography/computed tomography performed in early 2019 showed that both the primary metastasis in the left lower lobe (blue arrows) and the secondary hilar tumor, which is fluoro-2-deoxy-D-glucose avid (red arrows), were prostate-specific membrane antigen avid**

(3) exhibit clonal transformation to glycolytic CRPC, without neuroendocrine differentiation, and (4) the latter can take place without modification of the metabolic characteristics and hormone responsiveness of the primary metastatic focus.

## CONCLUSION

Modern imaging will continue to improve our understanding of PrCa progression. It is expected that in the next few years studies will identify the specific genomic signatures that guide metastatic behavior in prostate cancer.<sup>[9]</sup> Early detection with improved imaging techniques opens avenues for local management of such lesions with surgery or radiotherapy.<sup>[8]</sup> Accrual of such patients to clinical trials and biospecimen collection is crucial in achieving a better understanding and improved management of this disease. The reported case illustrates the validity of utilization of ADT and modern anti-androgen therapy as well as the on-going investigation of stereotactic body radiotherapy in oligometastatic PrCa.

## Acknowledgments

We thank Drs. H. Lukka\* and S. Hotte# for valuable input in the clinical management of this case and Dr. Georgia Douvi\* for support with preparation and submission of this manuscript. Divisions \*Radiation Oncology and #Medical Oncology, Juravinski Cancer Center, Hamilton, Ontario, Canada. This

publication has been reviewed and approved by the Hamilton integrated Research Ethics Board (HiREB).

## Declaration of patient consent

The authors certify that they have obtained all appropriate patient consent forms. In the form the patient(s) has/have given his/her/their consent for his/her/their images and other clinical information to be reported in the journal. The patients understand that their names and initials will not be published and due efforts will be made to conceal their identity, but anonymity cannot bechrological order guaranteed.

## Financial support and sponsorship

Nil.

## Conflicts of interest

There are no conflicts of interest.

## REFERENCES

- Han S, Woo S, Kim YJ, Suh CH. Impact of  $^{68}\text{Ga}$ -PSMA PET on the management of patients with prostate cancer: A systematic review and meta-analysis. *Eur Urol* 2018;74:179-90.
- Perera M, Murphy D, Lawrentschuk N. Prostate-specific membrane antigen positron emission tomography/computed tomography in locally advanced, recurrent, and metastatic prostate cancer. *JAMA Oncol* 2018;4:748-9.
- Gonzalez-Menendez P, Hevia D, Mayo JC, Sainz RM. The dark side of glucose transporters in prostate cancer: Are they a new feature to characterize carcinomas? *Int J Cancer* 2018;142:2414-24.
- Pertega-Gomes N, Felisbino S, Massie CE, Vizcaino JR, Coelho R, Sandi C, et al. A glycolytic phenotype is associated with prostate cancer progression and aggressiveness: A role for monocarboxylate transporters as metabolic targets for therapy. *J Pathol* 2015;236:517-30.
- Seniaray N, Verma R, Belho E, Malik D, Mahajan H. Diffuse pulmonary metastases from prostate cancer on  $^{68}\text{Ga}$  PSMA PET/CT. *Clin Nucl Med* 2019;44:898-900.
- Ost P, Reynders D, Decaestecker K, Fonteyne V, Lumen N, De Bruycker A, et al. Surveillance or metastasis-directed therapy for oligometastatic prostate cancer recurrence: A prospective, randomized, multicenter phase II trial. *J Clin Oncol* 2018;36:446-53.
- Gago JP, Câmara G, Dionísio J, Opinião A. Pulmonary metastasis as sole manifestation of relapse in previously treated localised prostate cancer: Three exceptional case reports. *Ecancermedalscience* 2016;10:645.
- Ciriaco P, Briganti A, Bernabei A, Gandaglia G, Carretta A, Viola C, et al. Safety and early oncologic outcomes of lung resection in patients with isolated pulmonary recurrent prostate cancer: A single-center experience. *Eur Urol* 2019;75:871-4.
- Sartor O, de Bono JS. Metastatic prostate cancer. *N Engl J Med* 2018;378:645-57.